INTERNATIONAL JOURNAL OF
NUMERICAL ANALYSIS AND MODELING
Volume 17, Number 1, Pages 54–67

CONFORMING HARMONIC FINITE ELEMENTS ON THE HSIEH-CLOUGH-TOCHER SPLIT OF A TRIANGLE

TATYANA SOROKINA AND SHANGYOU ZHANG

Abstract. We construct a family of conforming piecewise harmonic finite elements on triangulations. Because the dimension of harmonic polynomial spaces of degree $\leq k$ is much smaller than the one of the full polynomial space, the triangles in the partition must be refined in order to achieve optimal order of approximation power. We use the Hsieh-Clough-Tocher split: the barycenter of each original triangle is connected to its three vertices. Depending on the polynomial degree k, the original triangles have some minor restrictions which can be easily fulfilled by small perturbations of some vertices of the original triangulation. The optimal order of convergence is proved for the conforming harmonic finite elements, and confirmed by numerical computations. Numerical comparisons with the standard finite elements are presented, showing advantages and disadvantages of the harmonic finite element method.

Key words. Harmonic polynomial, conforming finite element, triangular grid, Hsieh-Clough-Tocher, Laplace equation.

1. Introduction

Standard finite element methods use the full space P_k of polynomials of total degree $\leq k$, or its enrichment by the so-called bubble functions, on each element (e.g. triangle or tetrahedron) for solving partial differential equations. That is, to reach the optimal order of approximation, the traditional finite element space must contain the full space P_k locally, cf. [2, 4, 5, 6, 7, 8, 9, 10, 14, 15, 16, 17].

Instead of using the full polynomial space P_k, in this work we use the harmonic polynomials $P_{k,\text{harm}}$ to construct conforming finite elements of optimal order for approximating only harmonic solutions. A harmonic polynomial p in two variables is a harmonic function, i.e., $\Delta p = p_{xx} + p_{yy} = 0$. For each $k > 0$, there are only two harmonic polynomials of exact degree k in two variables. They are the real and the imaginary part of the analytic polynomial $z^k = (x + iy)^k$. The dimension of $P_{k,\text{harm}}$ is $2k + 1$ as opposite to $(k + 1)(k + 2)/2$ for the dimension of P_k. But the order of convergence of the corresponding finite elements is the same.

We solve the following boundary value problem that has a harmonic solution:

$$\begin{aligned} -\Delta u &= 0, \quad \text{in } \Omega, \\ u &= f, \quad \text{on } \partial\Omega, \end{aligned} \tag{1}$$

where Ω is a bounded polygonal domain in $\mathbb{R}^2$. If the equation (1) has a non-zero function g on the right-hand side, i.e., $-\Delta u = g$, then the Fourier transform method can be used to find a solution u_1 such that $-\Delta u_1 = g$ without any boundary condition. Next the problem is reduced to a homogeneous problem with the boundary condition f in (1) replaced by $f - u_1$. The solution to the original problem is given by $u + u_1$.

The projection of $P_{k,\text{harm}}$ on a line in $\mathbb{R}^2$ is the full space of univariate polynomials of degree $\leq k$. Thus, to construct a harmonic finite element, we need $k + 1$ degrees of freedom on each edge in the triangulation in order to have a continuous finite

Received by the editors April 16, 2019.
2000 *Mathematics Subject Classification.* 65N30, 65N15.

element space (conforming finite element). This would lead at least $3k$ degrees of freedom in each triangle, see Fig. 1. But the dimension of $P_{k,\text{harm}}$ is only $2k+1$. Thus, to construct 2D conforming harmonic finite elements on a triangulation, one has to split the original triangles. In this work, we construct $P_{k,\text{harm}}$ conforming finite elements on Hsieh-Clough-Tocher (H-C-T) refinements of triangulations. An H-C-T refinement is obtained by connecting the barycenter of each triangle to its three vertices. Thus, each macro-triangle in the original triangulation is split into three subtriangles, and we have to work with three harmonic polynomials on one H-C-T macro-triangle. There are $3(2k+1) = 6k+3$ polynomial coefficients to be determined. For the continuity along three internal edges, we impose $3(k+1)-1 = 3k+2$ linear equations. By specifying the nodal values on the boundary and at the barycenter we obtain $3k+1$ equations. The total number of equations, $3k+2+3k+1$, is equal to the number of polynomial coefficients to be determined.

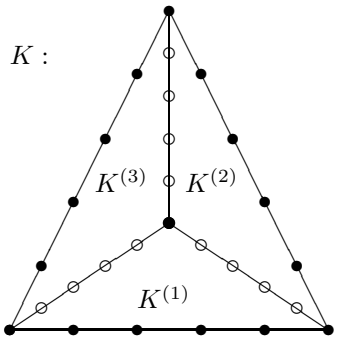

FIGURE 1. In K, $\bullet$ denotes a degree of freedom of $P_{5,\text{harm}}$ finite element; $\circ$ denotes a continuity constraints.

However, these equations may not have (unique) solutions. We show that, in general, this depends on the geometry of macro-triangles. In particular, for $k = 2$, there are no geometric constraints. For $k = 3$, only isosceles triangles are not allowed. For each k afterward, there is an an additional restriction that a certain polynomial function of the three angles does not vanish. Nevertheless, the prohibited combinations of the angles form a zero measure subset of the domain of the angles. So, in computation, we simply perturb one of the three vertices of a triangle if the computer fails to generate basis functions on this macro-triangle.

We prove a special case of the Bramble-Hilbert lemma [3] for approximating harmonic functions by harmonic polynomials. Using the lemma, we show that the harmonic finite elements converge at the optimal order, when solving (1). In the last section, we numerically test the harmonic finite elements of degree 2 to 6, confirming the theoretical results. In addition, numerical comparisons with the standard finite elements are presented. In an earlier work [12], we constructed a $P_{2,\text{harm}}$ conforming finite element on macro-rectangles, and a $P_{2,\text{harm}}$ nonconforming finite element on general non-refined triangulations.

2. Definition of harmonic finite elements

Let $\mathcal{M}_h = \cup_{K\in\mathcal{T}_h} K$ be a quasi-uniform triangulation of size h on the polygonal domain $\Omega \subset \mathbb{R}^2$. Depending on the harmonic polynomial degree k, cf. Theorem 2.1 below, we may need to perturb some internal vertices a little to form a new triangulation $\tilde{\mathcal{M}}_h$ in the computation. Each triangle K in $\tilde{\mathcal{M}}_h$ is subdivided into

three triangles by connecting its barycenter with the three vertices: $K^{(1)}$, $K^{(2)}$ and $K^{(3)}$, see Fig. 1. We call this refinement of the original triangulation a *Hsieh-Clough-Tocher split*: $\mathcal{T}_h = \cup_{K\in\breve{\mathcal{M}}_h} \cup_{l=1}^{3} K^{(l)}$.

The P_k harmonic finite element space or $P_{k,\mathrm{harm}}$ finite element space is defined by

$$V_h = \{v_h \in H^1(\Omega) \mid \quad v_h|_{K^{(l)}} \in P_{k,\mathrm{harm}} \text{ for all } K^{(l)} \in \mathcal{T}_h\}, \tag{2}$$

where $P_{k,\mathrm{harm}}$ is the space of harmonic polynomials of degree $\le k$ in two variables. We give a constructive definition of (2) next by specifying a nodal basis of the linear vector space. As in Fig. 1, on a single triangle $K := \Delta \mathbf{x}_1\mathbf{x}_2\mathbf{x}_3$, the interpolation nodes are

$$\mathcal{I}_K := \Big\{ \frac{1}{3}\sum_{l=1}^{3} \mathbf{x}_l,\ \frac{(k-j)\mathbf{x}_l + j\mathbf{x}_{l+1}}{k},\ j = 1,\dots,k,\ l = 1,2,3, \Big\}$$

where $\mathbf{x}_{l+3} := \mathbf{x}_l$. Let

$$\mathcal{I} = \bigcup_{K\in\mathcal{T}_h} \mathcal{I}_K.$$

With zero boundary value, the interior finite element space is defined as

$$V_h^0 = \{v_h \in V_h \mid v_h(\mathbf{y}) = 0 \text{ for all } \mathbf{y} \in \mathcal{I} \cap \partial\Omega \ \}.$$

The harmonic finite element problem for solving (1) reads: Find $u_h \in V_h$ such that $u_h(\mathbf{y}) = u(\mathbf{y})$ at all boundary nodes $\mathbf{y} \in \mathcal{I}$, and

$$a_h(u_h, v_h) = 0, \qquad \forall v_h \in V_h^0, \tag{3}$$

where the discrete bilinear form

$$a_h(u_h, v_h) = \sum_{K\in\mathcal{T}_h} \int_K \nabla u_h \cdot \nabla v_h \ d\mathbf{x}.$$

Theorem 2.1. *Let $\{z_m\}_{m=1}^{3k+1}$ be arbitrary real numbers, let K be a triangle with three angles $\theta_1 \ge \theta_2 \ge \theta_3$. There exists a unique $u_h \in V_h$ satisfying the interpolation conditions*

$$u_h(\mathbf{y}_i) = z_m, \quad \forall \quad \mathbf{y}_m \in \mathcal{I}_K, \tag{4}$$

if the three angles of K satisfy the constraints

$$\begin{aligned} t_j(\theta_1,\theta_2) :=& \frac{p_{2j+1}(-2\cot\theta_1 - \cot\theta_2, 1)}{p_{2j+1}(\cot\theta_1 + 2\cot\theta_2, 1)} \cdot \frac{p_{2j+1}(-2\cot\theta_2 - \cot\theta_3, 1)}{p_{2j+1}(\cot\theta_2 + 2\cot\theta_3, 1)} \\ &\cdot \frac{p_{2j+1}(-2\cot\theta_3 - \cot\theta_1, 1)}{p_{2j+1}(\cot\theta_3 + 2\cot\theta_1, 1)} \neq 1, \quad j = 2, ..., k, \end{aligned} \tag{5}$$

where

$$p_{2j+1}(x, y) = \mathrm{Im}\left((x + iy)^j\right).$$

Proof. On the three triangles $K^{(l)}$, $l = 1, 2, 3$, in the H-C-T split of K, three harmonic polynomials $u_h^l := u_h|_{K^{(l)}}$ of degree $\le k$ have a total of $6k + 3$ coefficients to be determined. By the interpolation conditions (4), we obtain $3k + 1$ linear equations for the above unknown coefficients. Then, by the continuity along the three internal edges (E_l in Fig. 2), we get $3(k + 1) - 1 = 3k + 2$ linear equations (one redundant constraint at the barycenter.) This yields a square system of linear equations. The uniqueness of its solution would provide the existence of the solution. Therefore, we need to show that u_h vanishes on K if $z_m = 0$ for all $m = 1, \dots, 3k + 1$.

Because being harmonic is invariant under rigid motion transformations, we may assume the triangle K is located as in Fig. 2, where l_1, l_2 and l_3 are the lengths of the three edges opposite to the vertices $\mathbf{x}_1$, $\mathbf{x}_2$, and $\mathbf{x}_3$, respectively, and E_1, E_2 and E_3 are the internal edges. Since $u_h^{(1)}$ is identically zero on the edge $[\mathbf{x}_2, \mathbf{x}_3]$, i.e., $u_h^{(1)}(x,0) \equiv 0$, we can write $u_h^{(1)}(x,y) = yq_{k-1}(x,y)$ where q_{k-1} is a polynomial of degree $\leq k-1$. Therefore, if we write $u_h^{(1)}(x,y)$ as a linear combination of the harmonic basis polynomials, we only have the imaginary part left:

$$u_h^{(1)}(x,y) = \sum_{j=1}^{k} a_j^{(1)} p_{2j+1}(x,y), \quad \text{where} \quad p_{2j+1}(x,y) = \operatorname{Im}\big((x+iy)^j\big).$$

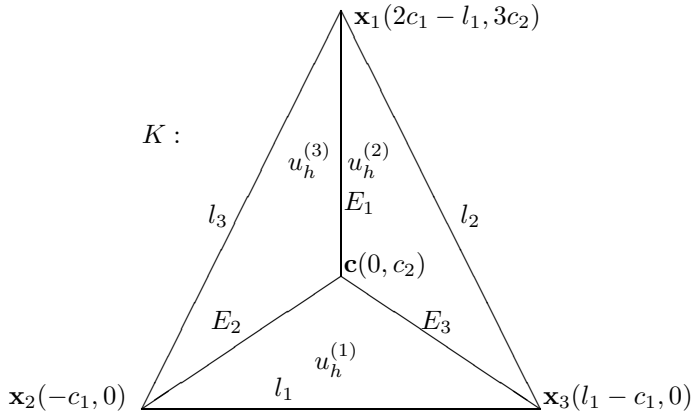

FIGURE 2. Shifted and rotated version of K.

Parametric equations for the line segments E_2 and E_3 are:

$$\begin{aligned} E_2: &\quad \mathbf{r}_2(t) = \langle -c_1 t, c_2(1-t)\rangle, \quad 0 \leq t \leq 1, \\ E_3: &\quad \mathbf{r}_3(t) = \langle (l_1 - c_1)t, c_2(1-t)\rangle, \quad 0 \leq t \leq 1. \end{aligned}$$

Next we rotate and shift K so that the edge l_3 is horizontal, and the first coordinate of the split point is zero. We denote this version of K by $\tilde{K}$, see Fig. 3. Since $\tilde{u}_h^{(3)}(x,0) \equiv 0$, we can write

$$\tilde{u}_h^{(3)}(x,y) = \sum_{j=1}^{k} \tilde{a}_j^{(3)} p_{2j+1}(x,y), \quad \text{where} \quad p_{2j+1}(x,y) = \operatorname{Im}\big((x+iy)^j\big).$$

Note that the old parameters c_1 and c_2 become c_3 and c_4 after the rotation, and the parametric equations of $\tilde{E}_2$ and $\tilde{E}_1$, under the rotated coordinate system in Fig. 3 are

$$\begin{aligned} \tilde{E}_2: &\quad \tilde{\mathbf{r}}_2(t) = \langle (l_3 - c_3)t, c_4(1-t)\rangle, \quad 0 \leq t \leq 1, \\ \tilde{E}_1: &\quad \tilde{\mathbf{r}}_1(t) = \langle -c_3 t, c_4(1-t)\rangle, \quad 0 \leq t \leq 1. \end{aligned}$$

By the continuity conditions along the interior edges we have

$$u_h^{(1)}|_{E_2} = u_h^{(3)}|_{E_2} =: u(t), \quad \text{and} \quad \tilde{u}_h^{(1)}|_{\tilde{E}_2} = \tilde{u}_h^{(3)}|_{\tilde{E}_2} =: \tilde{u}(t).$$

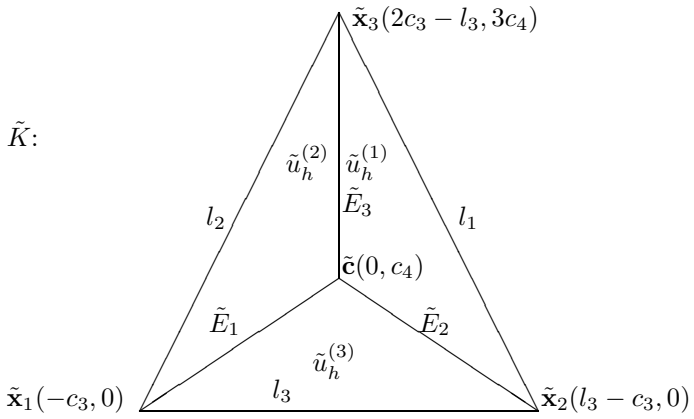

FIGURE 3. $\tilde{K}$, a rotated and shifted version of K in Fig. 2.

Note that since $\tilde{K}$ is a rotated version of K, the univariate polynomials $u(t)$ and $\tilde{u}(t)$ are identical. Therefore, we obtain

$$\tilde{u}_h^{(3)}((l_3 - c_3)t, c_4(1-t)) = u_h^{(1)}(-c_1 t, c_2(1-t)), \quad 0 \le t \le 1. \tag{6}$$

Finally, we rotate and shift K one more time to align l_2 with the y-axis as in Fig. 4. We denote this version of K by $\overline{K}$. Then $\overline{u}_h^{(2)}(x, 0) \equiv 0$, and, we can write

$$\overline{u}_h^{(2)}(x, y) = \sum_{j=1}^{k} \overline{a}_j^{(2)} p_{2j+1}(x, y), \quad \text{where} \quad p_{2j+1}(x, y) = \operatorname{Im}\big((x + iy)^j\big).$$

Using continuity along the remaining edges, and omitting some details for brevity, we arrive at two more continuity conditions:

$$\tilde{u}_h^{(3)}(-c_3 t, c_4(1-t)) = \overline{u}_h^{(2)}((l_2 - c_5)t, c_6(1-t)), \quad 0 \le t \le 1, \tag{7}$$

$$u_h^{(1)}((l_1 - c_1)t, c_2(1-t)) = \overline{u}_h^{(2)}(-c_5 t, c_6(1-t)), \quad 0 \le t \le 1. \tag{8}$$

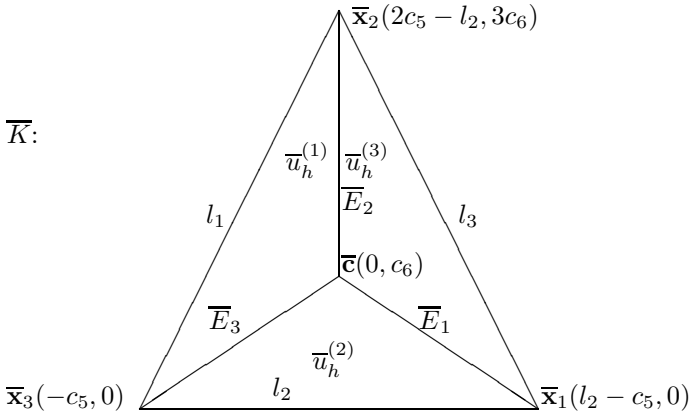

FIGURE 4. $\overline{K}$, a rotated and shifted version of K in Fig. 2.

Comparing the coefficients of t^k in (6), (7) and (8) we obtain

$$
\begin{aligned}
a_k^{(1)} p_{2k+1}(-c_1,-c_2) &= \tilde{a}_k^{(3)} p_{2k+1}(l_3-c_3,-c_4),\\
\tilde{a}_k^{(3)} p_{2k+1}(-c_3,-c_4) &= \overline{a}_k^{(2)} p_{2k+1}(l_2-c_5,-c_6),\\
\overline{a}_k^{(2)} p_{2k+1}(-c_5,-c_6) &= a_k^{(1)} p_{2k+1}(l_1-c_1,-c_2).
\end{aligned} \tag{9}
$$

Since c_2, c_4, and c_6 are not zeros, we can use the homogeneity of p_{2k+1} to obtain

$$
\begin{aligned}
a_k^{(1)} c_2^{-k} p_{2k+1}(c_1/c_2,1) &= \tilde{a}_k^{(3)} c_4^{-k} p_{2k+1}((c_3-l_3)/c_4,1),\\
\tilde{a}_k^{(3)} c_4^{-k} p_{2k+1}(c_3/c_4,1) &= \overline{a}_k^{(2)} c_6^{-k} p_{2k+1}((c_5-l_2)/c_6,1),\\
\overline{a}_k^{(2)} c_6^{-k} p_{2k+1}(c_5/c_6,1) &= a_k^{(1)} c_2^{-k} p_{2k+1}((c_1-l_1)/c_2,1).
\end{aligned} \tag{10}
$$

To solve (10), we need to invoke the geometry of K. Let θ_i be the angle at $\mathbf{x}_i$, $i=1,2,3$. Using the lengths of the edges of K, and the fact that $(0,c_2)$ is the barycenter of K, see Fig. 2, we compute

$$
\begin{aligned}
c_1 &= \frac{3l_1^2+l_3^2-l_2^2}{6l_1}, \quad l_1-c_1 = \frac{3l_1^2+l_2^2-l_3^2}{6l_1},\\
c_2 &= \frac{\sqrt{2(l_1^2l_2^2+l_2^2l_3^2+l_3^2l_1^2)-l_1^4-l_2^4-l_3^4}}{6l_1} = \frac{4|K|}{6l_1},\\
\frac{c_1}{c_2} &= \frac{2l_1(l_2\cos\theta_3+2l_3\cos\theta_2)}{2l_1l_3\sin\theta_2} = \cot\theta_3+2\cot\theta_2,\\
\frac{l_1-c_1}{c_2} &= \frac{2l_1(2l_2\cos\theta_3+l_3\cos\theta_2)}{2l_1l_3\sin\theta_2} = 2\cot\theta_3+\cot\theta_2,
\end{aligned}
$$

with similar expressions for c_3/c_4, $(l_3-c_3)/c_4$, c_5/c_6, and $(l_2-c_5)/c_6$. Using (5) in (10) we obtain

$$
a_k^{(1)} = a_k^{(1)} t_k(\theta_1,\theta_2).
$$

Therefore, $a_k^{(1)}=0$ if $t_k(\theta_1,\theta_2)\neq 1$ or $t_k^{-1}(\theta_1,\theta_2)\neq 1$. We continue by induction on j: assuming that $a_i^{(1)}=0$ for all $i\geq j$, and comparing the polynomial coefficients of t^{j-1} in (6) and (7), we obtain

$$
a_j^{(1)} = a_j^{(1)} t_j(\theta_1,\theta_2), \quad j=2,...,k.
$$

Therefore, $a_j^{(1)}=0$ if $t_j(\theta_1,\theta_2)\neq 1$ for $j=2,\ldots,k$. Note that the coefficients in front of t^0 in both $\tilde{u}_h^{(3)}((l_3-c_3)t, c_4(1-t))$ and $u_h^{(1)}(-c_1t, c_2(1-t))$ must be zero, because of the interpolating condition at the split point of the H-C-T split. This yields $a_1^{(1)}c_2 = \tilde{a}_1^{(3)}c_4 = 0$. Since c_2 and c_4 are both non-zero, we have $a_1^{(1)}=\tilde{a}_1^{(3)}=0$. Comparing the remaining coefficients in front of t, we obtain

$$
-a_1^{(1)}c_2 = -\tilde{a}_1^{(3)}c_4 = 0,
$$

which explains why $t_j(\theta_1,\theta_2)\neq 1$ does not need to hold for $j=1$. Thus, if $t_j(\theta_1,\theta_2)\neq 1$, for $j=2,\ldots,k$, holds then all $a_j^{(1)}=0$, $u_h^{(1)}\equiv 0$, and $u_h\equiv 0$. This completes the proof. ∎

Remark 2.1. *In Theorem 2.1, if $k = 2$, then $p_5 = xy$, and*

$$t_2(\theta_1,\theta_2) = \frac{(-2\cot\theta_1 - \cot\theta_2)}{(\cot\theta_1 + 2\cot\theta_2)} \cdot \frac{(-2\cot\theta_2 - \cot\theta_3)}{(\cot\theta_2 + 2\cot\theta_3)} \cdot \frac{(-2\cot\theta_3 - \cot\theta_1)}{(\cot\theta_3 + 2\cot\theta_1)} = -\frac{l_1 + l_{13}}{l_1 + l_{12}} \cdot \frac{l_2 + l_{21}}{l_2 + l_{23}} \cdot \frac{l_3 + l_{32}}{l_2 + l_{31}},$$

where l_{jk} is the signed projection of l_k on the edge l_j. If all angles are non-obtuse, all $l_j + l_{jk} > 0$ and $t_2(\theta_1,\theta_2) < 0$, i.e., (5) holds. If the largest angle $\theta_1 > \pi/2$ and l_2 (the edge opposite θ_2) is much larger than l_3, only one term, $l_3 + l_{32} = l_3 + l_2\cos\theta_1$, will be negative while the other 5 terms are non-negative. For this fixed $\theta_1 > \pi/2$, the function $t_2(\theta_1,\theta_2)$ is an increasing function of θ_2 (by checking the derivative.) It is easy to see that $t_2(\theta_1,(\pi-\theta_1)/2) = -1$ when $\theta_2 = \theta_3$, and $t_2(\theta_1,\pi-\theta_1) = 1$ when $\theta_3 = 0$. Thus, for any non-degenerate triangle K, $t_2(\theta_1,\theta_2) < 1$. (5) always holds for $k = 2$, independent on the geometry of K. That is, for quadratic harmonic finite elements, there is no restriction on the triangles in $\mathcal{M}_h$. Additionally, in [13]*, we show that even if the split point of the H-C-T split is not a barycenter, for quadratic harmonic finite elements, there is still no restriction on the geometry. This is in striking contrast to higher degree harmonic splines.*

Remark 2.2. *In Theorem 2.1, if $k = 3$, we need, in addition to $t_2(\theta_1,\theta_2) < 1$ in Remark 2.1, to consider $p_7 = 3x^2y - y^3$, i.e.,*

$$t_3(\theta_1,\theta_2) = \frac{3(2\cot\theta_1 + \cot\theta_2)^2 - 1}{3(\cot\theta_1 + 2\cot\theta_2)^2 - 1} \cdot \frac{3(2\cot\theta_2 + \cot\theta_3)^2 - 1}{3(\cot\theta_2 + 2\cot\theta_3)^2 - 1} \cdot \frac{3(2\cot\theta_3 + \cot\theta_1)^2 - 1}{3(\cot\theta_3 + 2\cot\theta_1)^2 - 1} \neq 1.$$

Clearly, if the triangle is isosceles, the above fraction is simplified to 1. In the Appendix, we show directly that in this case the cubic harmonic finite element is not uni-solvent.

Remark 2.3. *It is interesting to note, that on the standard triangle, no matter how we choose the split point in the H-C-T split, the quartic harmonic finite element is not uni-solvent, see the Appendix.*

Lemma 2.1. *If every $K \in \mathcal{T}_h$ satisfies* (5)*, the finite element problem* (3) *has a unique solution.*

Proof. The problem (3) is a square system of linear equations. The uniqueness of its solution implies existence. Let u_h be a solution of (3) with zero boundary value $u_h = 0$ at the boundary nodes in $\mathcal{I}$. Then $a_h(u_h,u_h) = 0$ implies $\nabla u_h = 0$ on each triangle. So u_h is a constant function on each triangle. Because u_h is continuous, u_h is a global P_0 function on the whole domain. By the boundary condition, $u_h = 0$. ∎

3. Convergence theory

We start by proving a version of Bramble-Hilbert lemma [3] for the harmonic polynomial space.

Lemma 3.1. *For any harmonic function $u \in H^{k+1}(K)$ on a triangle K, there is a harmonic polynomial q_k of degree $\leq k$ such that*

$$\sum_{j=0}^{1} h^j \|u - q_k\|_{H^j(K)} \leq Ch^{k+1}|u|_{H^{k+1}(K)}. \tag{11}$$

Proof. Let K be an arbitrary shape-regular triangle of size h, and let B be its inscribed circle. For any harmonic function $u \in H^{k+1}(K)$ on K, let $Q^k u$ be the Taylor polynomial of degree k of u averaged over B. Then from Bramble-Hilbert Lemma 4.3.8 in [4], it follows that

$$\sum_{j=0}^{1} h^j \|u - Q^k u\|_{H^j(K)} \leq C h^{k+1} |u|_{H^3(K)}. \tag{12}$$

In order to prove our result, we need to show that $q_k := Q^k u$ is a harmonic polynomial. Indeed, from Proposition 4.1.17 in [4], it follows that

$$\Delta(Q^k u) = Q^{k-2}(\Delta u) = 0,$$

and the proof is complete. ∎

Theorem 3.1. *Let u and u_h be the exact solution of* (1) *and the finite element solution of* (3)*, respectively. Then*

$$\|u - u_h\|_1 \leq C h^k \|u\|_{k+1}. \tag{13}$$

Proof. Let I_h be the Scott-Zhang interpolation operator of [11] to the space V_h. Then $u_h = I_h u$ on the boundary, and

$$\begin{aligned} \|u - I_h u\|_1^2 &\leq 2 \sum_{K \in \mathcal{T}_h} \|u - q_k\|_{1,K}^2 + \|I_h(u - q_k)\|_{1,K}^2 \\ &\leq C \sum_{K \in \mathcal{T}_h} \|u - q_k\|_{1,K}^2 \leq C h^{2k} \|u\|_{k+1}^2, \end{aligned}$$

where q_k is the harmonic polynomial from (11) on each triangle K in $\mathcal{M}_h$. Next we define an auxiliary solution: $u_b|_{\partial\Omega} = I_h f$ and

$$a(u_b, v) = 0 \quad \forall v \in H_0^1(\Omega). \tag{14}$$

Assuming the domain is regular enough, we obtain

$$\begin{aligned} \|u - u_b\|_1 &\leq C \|u - I_h f\|_{H^{1/2}(\partial\Omega)} \\ &\leq C h^k \|u\|_{H^{k+1/2}(\partial\Omega)} \leq C h^k \|u\|_{k+1}. \end{aligned} \tag{15}$$

Note that, on the boundary the harmonic interpolation is the full univariate P_k-polynomial interpolation. Let the solution u_h of (3) be decomposed into two parts as follows: $u_h = u_{1,h} + u_{0,h}$, where $u_{0,h} \in V_h \cap H_0^1(\Omega)$ and $u_{1,h}$ is equal to u_h on the domain boundary, and has zero nodal values at all internal nodes of V_h. Then we can define $u_0 := u_b - u_{1,h}$. By (3) and (14), we obtain

$$a(u_0 - u_{0,h}, v_h) = a(u_b - u_h, v_h) = 0, \quad \forall v_h \in V_h \cap H_0^1(\Omega).$$

Therefore,

$$|u_0 - u_{0,h}|_1^2 = a(u_0 - u_{0,h}, u_0 - I_h u_0) \leq |u_0 - u_{0,h}|_1 |u_0 - I_h u_0|_1. \tag{16}$$

Using (16) and (15) we complete the proof as follows

$$\begin{aligned} \|u - u_h\|_1 &\leq \|u - u_b\|_1 + \|u_b - u_h\|_1 = \|u - u_b\|_1 + \|u_0 - u_{0,h}\|_1 \\ &\leq \|u - u_b\|_1 + \|u_0 - I_h u_0\|_1 = \|u - u_b\|_1 + \|u_b - I_h u_b\|_1 \\ &\leq 2\|u - u_b\|_1 + \|u - I_h u\|_1 + \|I_h(u - u_b)\|_1 \\ &\leq C\|u - u_b\|_1 + \|u - I_h u\|_1 \leq C h^k \|u\|_{k+1}. \end{aligned}$$

∎

4. Numerical tests

Let the domain of the boundary value problem (1) be $\Omega = (0,1)^2$. The exact solution is $u(x,y) = e^x \sin y$. We chose a family of perturbed uniform grids, shown in Figure 5, for all harmonic finite element methods and for the P_k finite element methods.

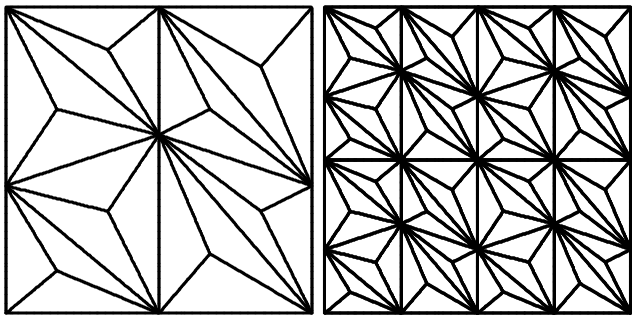

FIGURE 5. The first two level grids.

We solve problem (1) first by the harmonic P_2 finite element method and by the P_2 Lagrange finite element method. The errors and the orders of convergence are listed in Table 1. On the last level, the P_2 harmonic element space has about half degrees of freedom of that of the P_2 Lagrange finite element space. The computing time is about 1/20 of that of the P_2 Lagrange element. But the accuracy is much higher (about 1/2 error). In theory, if the boundary condition is interpolated appropriately, by Ceá's lemma, the semi-H^1 error, $|u - u_h|_1$ (not the $|I_h u - u_h|_1$ here), of the P_2 Lagrange element would be smaller than that of the P_2 harmonic element, as the latter is a subspace.

TABLE 1. The error $e_h = I_h u - u_h$ and the order of convergence, by the P_2 harmonic finite element and by the P_2 Lagrange finite element.

grid	$\|e_h\|_0$	h^n	$\|e_h\|_1$	h^n	$\|e_h\|_0$	h^n	$\|e_h\|_1$	h^n
	P_2 harmonic element				P_2 Lagrange element			
1	0.680e-03	0.0	0.834e-02	0.0	0.109e-02	0.0	0.270e-01	0.0
2	0.715e-04	3.3	0.202e-02	2.0	0.124e-03	3.1	0.653e-02	2.0
3	0.837e-05	3.1	0.499e-03	2.0	0.149e-04	3.1	0.160e-02	2.0
4	0.103e-05	3.0	0.125e-03	2.0	0.183e-05	3.0	0.395e-03	2.0
5	0.128e-06	3.0	0.312e-04	2.0	0.227e-06	3.0	0.982e-04	2.0
6	0.160e-07	3.0	0.779e-05	2.0	0.283e-07	3.0	0.245e-04	2.0
7	0.200e-08	3.0	0.195e-05	2.0	0.353e-08	3.0	0.611e-05	2.0
8	0.250e-09	3.0	0.488e-06	2.0	0.440e-09	3.0	0.153e-05	2.0
	Last cpu: 32; dof=394241				Last cpu: 541; dof=787457			

Next we solve problem (1) again, by the harmonic P_3 finite element method and by the P_3 Lagrange finite element method. The errors and the orders of convergence are listed in Table 2. Again, both methods converge in the optimal order. But unlike the P_2 case, the P_3 harmonic finite element method is less accurate than the standard P_3 finite element method.

TABLE 2. The error $e_h = I_h u - u_h$ and the order of convergence, by the P_3 harmonic finite element and by the P_3 Lagrange finite element.

grid	$\|e_h\|_0$	h^n	$\|e_h\|_1$	h^n	$\|e_h\|_0$	h^n	$\|e_h\|_1$	h^n
	P_3 harmonic element				P_3 Lagrange element			
1	0.110E-02	0.0	0.273E-01	0.0	0.363E-04	0.0	0.954E-03	0.0
2	0.677E-04	4.0	0.360E-02	2.9	0.220E-05	4.0	0.124E-03	2.9
3	0.416E-05	4.0	0.456E-03	3.0	0.134E-06	4.0	0.155E-04	3.0
4	0.256E-06	4.0	0.571E-04	3.0	0.828E-08	4.0	0.195E-05	3.0
5	0.159E-07	4.0	0.716E-05	3.0	0.514E-09	4.0	0.243E-06	3.0
6	0.989E-09	4.0	0.895E-06	3.0	0.319E-10	4.0	0.304E-07	3.0
7	0.623E-10	4.0	0.112E-06	3.0	0.196E-11	4.0	0.380E-08	3.0
	Last cpu: 163; dof=148225				Last cpu: 285; dof=443137			

TABLE 3. The error $e_h = I_h u - u_h$ and the order of convergence, by the $P_4/P_5/P_6$ harmonic finite elements and by the $P_4/P_5/P_6$ Lagrange finite elements.

grid	$\|e_h\|_0$	h^n	$\|e_h\|_1$	h^n	$\|e_h\|_0$	h^n	$\|e_h\|_1$	h^n
	P_4 harmonic element				P_4 Lagrange element			
1	0.586E-02	0.0	0.198E+00	0.0	0.151E-05	0.0	0.541E-04	0.0
2	0.176E-03	5.1	0.120E-01	4.0	0.447E-07	5.1	0.327E-05	4.0
3	0.534E-05	5.0	0.727E-03	4.0	0.134E-08	5.1	0.199E-06	4.0
4	0.164E-06	5.0	0.446E-04	4.0	0.406E-10	5.0	0.122E-07	4.0
5	0.507E-08	5.0	0.276E-05	4.0	0.130E-11	5.0	0.759E-09	4.0
	Last cpu: 761; dof=12545				Last cpu: 15; dof=49409			
	P_5 harmonic element				P_5 Lagrange element			
1	0.155E-02	0.0	0.523E-01	0.0	0.755E-07	0.0	0.365E-05	0.0
2	0.193E-04	6.3	0.131E-02	5.3	0.109E-08	6.1	0.108E-06	5.1
3	0.279E-06	6.1	0.381E-04	5.1	0.162E-10	6.1	0.326E-08	5.0
4	0.358E-07	3.0	0.117E-05	5.0	0.271E-12	5.9	0.100E-09	5.0
	Last cpu: 703; dof=4001				Last cpu: 7; dof=19361			
	P_6 harmonic element				P_6 Lagrange element			
1	0.110E-03	0.0	0.371E-02	0.0	0.174E-08	0.0	0.115E-06	0.0
2	0.702E-06	7.3	0.475E-04	6.3	0.131E-10	7.1	0.173E-08	6.1
3	0.185E-06	1.9	0.153E-05	5.0	0.108E-12	6.9	0.264E-10	6.0
	Last cpu: 447; dof=1249				Last cpu: 3; dof=7009			

We then solve problem (1) by the harmonic $P_4/P_5/P_6$ finite element methods and by the $P_4/P_5/P_6$ Lagrange finite element methods. The errors and the orders of convergence are listed in Table 3. The harmonic $P_4/P_5/P_6$ finite element method converges in the optimal order only at the first few levels. Surprisingly, the errors of high order harmonic finite element method are much bigger than those of the standard Lagrange finite element method. This is due to very oscillatory basis functions in the high order harmonic finite element method. The current double-precision computers cannot evaluate such basis functions to the required accuracy. The other problem is to find a better, projected boundary condition, instead of

current nodal interpolated boundary condition. The harmonic finite element solution is sensitive to the boundary condition, while the full polynomial finite element solution is not. Further, the global condition number of high order harmonic finite element systems is so big that the number of iterations for the conjugate gradient method for solving the linear system of high order harmonic element equations is way beyond the number of unknowns. This can be seen from the cpu(computing) time comparing to that of the Lagrange elements, see Table 3. It is a further research topic to find relatively well conditioned basis for the harmonic finite element, i.e., to precondition the local and the global stiffness matrix.

Acknowledgements

This research was supported by NSFC projection 11571023 to Shangyou Zhang, and by the Simons Foundation #235411 to Tatyana Sorokina.

References

[1] P. Alfeld, and T. Sorokina, Linear Differential Operators on Bivariate Spline Spaces and Spline Vector Fields, BIT Numerical Mathematics, 56(1), 15-32, 2016.
[2] D. N. Arnold, D. Boffi and R. S. Falk, Approximation by quadrilateral finite elements. Math. Comp. 71 (2002), no. 239, 909-922.
[3] J. H. Bramble and S. R. Hilbert, Estimation of linear functionals on Sobolev spaces with applications to Fourier transforms and spline interpolation, SIAM J. Numer. Anal., 7 (1970), 113–124.
[4] S. C. Brenner and L. R. Scott, The mathematical theory of finite element methods. Third edition. Texts in Applied Mathematics, 15. Springer, New York, 2008.
[5] R. S. Falk, P. Gatto and P. Monk, Hexahedral H(div) and H(curl) finite elements. ESAIM Math. Model. Numer. Anal. 45 (2011), no. 1, 115-143.
[6] J. Hu, Y. Huang and S. Zhang, The lowest order differentiable finite element on rectangular grids, SIAM Num. Anal. 49 (2011), No 4, 1350–1368.
[7] J. Hu and S. Zhang, The minimal conforming H^k finite element spaces on R^n rectangular grids, Math. Comp. 84 (2015), no. 292, 563–579.
[8] J. Hu and S. Zhang, Finite element approximations of symmetric tensors on simplicial grids in R^n: the lower order case, Math. Models Methods Appl. Sci. 26 (2016), no. 9, 1649–1669.
[9] Y. Huang and S. Zhang, Supercloseness of the divergence-free finite element solutions on rectangular grids, Commun. Math. Stat. 1 (2013), no. 2, 143–162.
[10] L. L. Schumaker, T. Sorokina and A. J. Worsey, A C1 quadratic trivariate macro-element space defined over arbitrary tetrahedral partitions. J. Approx. Theory, 158 (2009), No. 1, 126–142.
[11] L.R. Scott and S. Zhang, Finite element interpolation of nonsmooth functions satisfying boundary conditions, Math. Comp. 54 (1990), 483–493.
[12] T. Sorokina and S. Zhang, Conforming and nonconforming harmonic finite elements, Applicable Analysis, accepted.
[13] T. Sorokina and S. Zhang, An inequality involving a triangle and an interior point and its application, submitted.
[14] S. Zhang, A C1-P2 finite element without nodal basis, M2AN 42 (2008), 175–192.
[15] S. Zhang, A family of 3D continuously differentiable finite elements on tetrahedral grids, Applied Numerical Mathematics, 59 (2009), no. 1, 219–233.
[16] S. Zhang, A family of differentiable finite elements on simplicial grids in four space dimensions, (Chinese) Math. Numer. Sin. 38 (2016), no. 3, 309–324.
[17] S. Zhang, A P4 bubble enriched P3 divergence-free finite element on triangular grids, Comput. Math. Appl. 74 (2017), no. 11, 2710–2722.

Appendix A. Properties of the vector spherical harmonics

A.1. Bernstein-Bézier techniques. We recall some basic Bernstein-Bézier techniques first. Let

$$b_i = b_i(\mathbf{x}) \quad \text{where} \quad i = 1, 2, 3,$$

denote the *barycentric coordinates* of a point $\mathbf{x} = (x^1, x^2)$ relative to a triangle $T = [\mathbf{x}_1, \mathbf{x}_2, \mathbf{x}_3]$ in $\mathbb{R}^2$, where $\mathbf{x}_i = (x_i^1, x_i^2)$. The barycentric coordinates are defined by the equation

$$\begin{bmatrix} x_1^1 & x_2^1 & x_3^1 \\ x_1^2 & x_2^2 & x_3^2 \\ 1 & 1 & 1 \end{bmatrix} \begin{bmatrix} b_1 \\ b_2 \\ b_3 \end{bmatrix} = \begin{bmatrix} x^1 \\ x^2 \\ 1 \end{bmatrix}.$$

Every polynomial p of degree $\leq k$ can be written uniquely in its *Bernstein-Bézier (BB-form)* as

$$p(\mathbf{x}) = \sum_{i+j+l=k} c_{ijl} B_{ijl}, \quad \text{where} \quad B_{ijl} = \frac{k!}{i!j!l!} b_1^i b_2^j b_3^l. \tag{A.1}$$

The coefficients c_{ijl} are called the *BB-coefficients* of p. Each such coefficient is uniquely associated with its *domain point* $\xi_{ijk} = (i\mathbf{x}_1 + j\mathbf{x}_2 + l\mathbf{x}_3)/k$, $i + j + l = k$, located in T. The points (ξ_{ijl}, c_{ijl}) are called the *control points* of p. If p is harmonic, an additional condition is imposed on the BB-coefficients, see [1]: for all $i + j + l = k - 2$,

$$\begin{aligned} &c_{i+2,j,l}||\mathbf{x}_3 - \mathbf{x}_2||^2 + 2c_{i+1,j+1,l}(\mathbf{x}_1 - \mathbf{x}_3) \cdot (\mathbf{x}_3 - \mathbf{x}_2) \\ &+ 2c_{i+1,j,l+1}(\mathbf{x}_2 - \mathbf{x}_1) \cdot (\mathbf{x}_3 - \mathbf{x}_2) + c_{i,j+2,l}||\mathbf{x}_1 - \mathbf{x}_3||^2 + \\ &+ 2c_{i,j+1,l+1}(\mathbf{x}_1 - \mathbf{x}_3) \cdot (\mathbf{x}_2 - \mathbf{x}_1) + c_{ijl+2}||\mathbf{x}_2 - \mathbf{x}_1||^2 = 0. \end{aligned} \tag{A.2}$$

A.2. Cubic harmonic spline on the H-C-T split of an isosceles triangle. Let $\Delta_{CT}(T)$ be the H-C-T split of T into three subtriangles T_1, T_2, and T_3 as in Fig. 6(left). On each triangle T_i, $i = 1, 2, 3$, we define a cubic polynomial p_i, $i = 1, 2, 3$, in two variables. Each p_i has ten domain points depicted as either black dots or empty circles in Figure 6(left). Note that the three BB-coefficients associated with the domain points on the interior edges are the same for the neighboring polynomials. Thus, the piecewise polynomial is continuous on T. The black dots correspond to the BB-coefficients that will be set to arbitrary values. For simplicity, we introduce the following notation: $v_i = \mathbf{x}_i - \mathbf{x}_0$, $i = 1, 2, 3$, $u_1 = v_2 - v_3$, $u_2 = v_3 - v_1$ and $u_3 = v_1 - v_2$. Then the condition (A.2) gives rise to a linear system of 9 equations with 9 unknowns corresponding to the open dots in Figure 6(left). The matrix associated with this system is:

$$\begin{bmatrix} u_3 \cdot u_3 & -2u_3 \cdot v_2 & 2u_3 \cdot v_1 & 0 & 0 & 0 & 0 & 0 & 0 \\ u_2 \cdot u_2 & 2u_2 \cdot v_3 & 0 & 0 & 0 & 0 & 0 & 0 & -2u_2 \cdot v_1 \\ 0 & 0 & -2u_3 \cdot v_2 & 2u_3 \cdot v_1 & u_3 \cdot u_3 & 0 & 0 & 0 & 0 \\ 0 & 0 & 0 & -2u_1 \cdot v_3 & u_1 \cdot u_1 & 2u_1 \cdot v_2 & 0 & 0 & 0 \\ 0 & 0 & 0 & 0 & 0 & -2u_1 \cdot v_3 & 2u_1 \cdot v_2 & u_1 \cdot u_1 & 0 \\ 0 & 0 & 0 & 0 & 0 & 0 & -2u_2 \cdot v_1 & u_2 \cdot u_2 & 2u_2 \cdot v_3 \\ -2u_3 \cdot v_2 & v_2 \cdot v_2 & -2v_1 \cdot v_2 & v_1 \cdot v_1 & 2u_3 \cdot v_1 & 0 & 0 & 0 & 0 \\ 0 & 0 & 0 & v_3 \cdot v_3 & -2u_1 \cdot v_3 & -2v_2 \cdot v_3 & v_2 \cdot v_2 & 2u_1 \cdot v_2 & 0 \\ 2u_2 \cdot v_3 & v_3 \cdot v_3 & 0 & 0 & 0 & 0 & v_1 \cdot v_1 & -2u_2 \cdot v_1 & -2v_1 \cdot v_3 \end{bmatrix}.$$

By rotating and scaling any isosceles triangle, we can place the barycenter (the split point) at the origin and assume that $v_1 = (-a, -1)$, $v_2 = (a, -1)$, and $v_3 = (0, 2)$. Direct computation shows that the determinant of the matrix above vanishes. Thus, a cubic harmonic finite element on the H-C-T split (coning off the barycenter) of an isosceles triangle is not uni-solvent, see also Remark 2.2. However, by shifting the split point it is possible to find a configuration that guarantees uni-solvency. This is in striking contrast with out next example, where no matter which split point is chosen, the finite element is not uni-solvent.

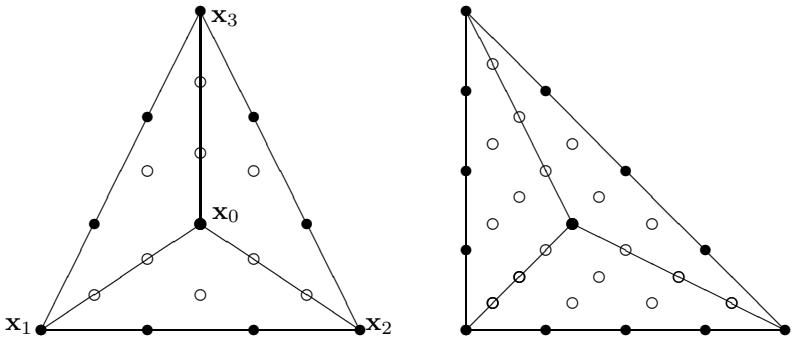

FIGURE 6. Domain points for the cubic (left) and the quartic (right) harmonic splines.

A.3. Quartic harmonic spline on the H-C-T split of a standard triangle. Let $\Delta_{CT}(T)$ be the H-C-T split of T into three subtriangles T_1, T_2, and T_3 as in Fig. 6(right). On each triangle T_i, $i = 1, 2, 3$, we define a quartic polynomial p_i, $i = 1, 2, 3$, in two variables. In this case, each p_i has 15 domain points depicted as either black dots or empty circles in Figure 6(right). The black dots correspond to the BB-coefficients that will be set to arbitrary values. Then the condition (A.2) gives rise to a linear system of 18 equations with 18 unknowns corresponding to the open dots in Figure 6(right). With the same notation as in the cubic case for u_i and v_i, $i = 1, 2, 3$, the first nine columns of the associated 18 by 18 matrix are:

$$\begin{bmatrix}
u_3\cdot u_3 & -2u_3\cdot v_2 & 2u_3\cdot v_1 & 0 & 0 & 0 & 0 & 0 & 0 \\
u_2\cdot u_2 & 2u_2\cdot v_3 & 0 & 0 & 0 & 0 & 0 & 0 & -2u_2\cdot v_1 \\
0 & 0 & -2u_3\cdot v_2 & 2u_3\cdot v_1 & u_3\cdot u_3 & 0 & 0 & 0 & 0 \\
0 & 0 & 0 & -2u_1\cdot v_3 & u_1\cdot u_1 & 2u_1\cdot v_2 & 0 & 0 & 0 \\
0 & 0 & 0 & 0 & 0 & -2u_1\cdot v_3 & 2u_1\cdot v_2 & u_1\cdot u_1 & 0 \\
0 & 0 & 0 & 0 & 0 & 0 & -2u_2\cdot v_1 & u_2\cdot u_2 & 2u_2\cdot v_3 \\
-2u_3\cdot v_2 & v_2\cdot v_2 & -2v_1\cdot v_2 & v_1\cdot v_1 & 2u_3\cdot v_1 & 0 & 0 & 0 & 0 \\
0 & 0 & 0 & v_3\cdot v_3 & -2u_1\cdot v_3 & -2v_2\cdot v_3 & v_2\cdot v_2 & 2u_1\cdot v_2 & 0 \\
2u_2\cdot v_3 & v_3\cdot v_3 & 0 & 0 & 0 & 0 & v_1\cdot v_1 & -2u_2\cdot v_1 & -2v_1\cdot v_3 \\
0 & u_3\cdot u_3 & 0 & 0 & 0 & 0 & 0 & 0 & 0 \\
0 & 0 & u_3\cdot u_3 & 0 & 0 & 0 & 0 & 0 & 0 \\
0 & 0 & 0 & u_3\cdot u_3 & 0 & 0 & 0 & 0 & 0 \\
0 & 0 & 0 & u_1\cdot u_1 & 0 & 0 & 0 & 0 & 0 \\
0 & 0 & 0 & 0 & 0 & u_1\cdot u_1 & 0 & 0 & 0 \\
0 & 0 & 0 & 0 & 0 & 0 & u_1\cdot u_1 & 0 & 0 \\
0 & 0 & 0 & 0 & 0 & 0 & u_2\cdot u_2 & 0 & 0 \\
0 & 0 & 0 & 0 & 0 & 0 & 0 & 0 & u_2\cdot u_2 \\
0 & u_2\cdot u_2 & 0 & 0 & 0 & 0 & 0 & 0 & 0
\end{bmatrix}.$$

And the last nine columns of the associated 18 by 18 matrix are:

$$\begin{bmatrix}
v_2\cdot v_2 & -2v_1\cdot v_2 & v_1\cdot v_1 & 0 & 0 & 0 & 0 & 0 & 0 \\
v_3\cdot v_3 & 0 & 0 & 0 & 0 & 0 & 0 & v_1\cdot v_1 & -2v_1\cdot v_3 \\
0 & v_2\cdot v_2 & -2v_1\cdot v_2 & v_1\cdot v_1 & 0 & 0 & 0 & 0 & 0 \\
0 & 0 & 0 & v_3\cdot v_3 & -2v_2\cdot v_3 & v_2\cdot v_2 & 0 & 0 & 0 \\
0 & 0 & 0 & 0 & v_3\cdot v_3 & -2v_2\cdot v_3 & v_2\cdot v_2 & 0 & 0 \\
0 & 0 & 0 & 0 & 0 & 0 & v_1\cdot v_1 & -2v_1\cdot v_3 & v_3\cdot v_3 \\
0 & 0 & 0 & 0 & 0 & 0 & 0 & 0 & 0 \\
0 & 0 & 0 & 0 & 0 & 0 & 0 & 0 & 0 \\
0 & 0 & 0 & 0 & 0 & 0 & 0 & 0 & 0 \\
-2u_3\cdot v_2 & 2u_3\cdot v_1 & 0 & 0 & 0 & 0 & 0 & 0 & 0 \\
0 & -2u_3\cdot v_2 & 2u_3\cdot v_1 & 0 & 0 & 0 & 0 & 0 & 0 \\
0 & 0 & -2u_3\cdot v_2 & 2u_3\cdot v_1 & 0 & 0 & 0 & 0 & 0 \\
0 & 0 & 0 & -2u_1\cdot v_3 & 2u_1\cdot v_2 & 0 & 0 & 0 & 0 \\
0 & 0 & 0 & 0 & -2u_1\cdot v_3 & 2u_1\cdot v_2 & 0 & 0 & 0 \\
0 & 0 & 0 & 0 & 0 & -2u_1\cdot v_3 & 2u_1\cdot v_2 & 0 & 0 \\
0 & 0 & 0 & 0 & 0 & 0 & -2u_2\cdot v_1 & 2u_2\cdot v_3 & 0 \\
0 & 0 & 0 & 0 & 0 & 0 & 0 & -2u_2\cdot v_1 & 2u_2\cdot v_3 \\
2u_2\cdot v_3 & 0 & 0 & 0 & 0 & 0 & 0 & 0 & -2u_2\cdot v_1
\end{bmatrix}.$$

Let (x, y) be the split point inside the standard triangle. Direct computation with $v_1 = (-x, -y)$, $v_2 = (1 - x, -y)$, $v_3 = (-x, 1 - y)$ shows that the determinant of the matrix above vanishes. Thus, it is impossible to construct a quartic harmonic

finite element on the H-C-T split of a standard triangle no matter what the split point is.

Department of Mathematics, Towson University, 7800 York Road, Towson, MD 21252, USA
E-mail: tsorokina@towson.edu
URL: https://tigerweb.towson.edu/tsorokin/

Department of Mathematical Sciences, University of Delaware, Newark, DE 19716, USA
E-mail: szhang@udel.edu
URL: http://www.math.udel.edu/∼szhang/